International Conference on Pattern Recognition
August 2002, I: 528-531


# Model-Based Brain and Tumor Segmentation

[1]Nathan Moon, [2]Elizabeth Bullitt, [4]Koen van Leemput, and [1,3]Guido Gerig

[1]Department of Computer Science, [2]Department of Surgery, [3]Department of Psychiatry
University of North Carolina, Chapel Hill, NC 27599, USA
[4] Radiology-ESAT/PSI, University Hospital Gasthuisberg, B-3000 Leuven, Belgium
email: gerig@cs.unc.edu

*Abstract*— **Combining image segmentation based on statistical classification with a geometric prior has been shown to significantly increase robustness and reproducibility. Using a probabilistic geometric model of sought structures and image registration serves both initialization of probability density functions and definition of spatial constraints. A strong spatial prior, however, prevents segmentation of structures that are not part of the model. In practical applications, we encounter either the presentation of new objects that cannot be modelled with a spatial prior or regional intensity changes of existing structures.**

**Our driving application is the segmentation of brain tissue and tumors from three-dimensional magnetic resonance imaging (MRI). We aim at both obtaining a high-quality segmentation of healthy tissue and a precise delineation of tumor boundaries. We present an extension to an existing expectation maximization segmentation (EM) algorithm that modifies a probabilistic brain atlas with individual subject's information about tumor location. This information is obtained from subtraction of post- and pre-contrast MRI and calculation of a posterior probability map for tumor. The new method handles both phenomena, space-occupying mass tumors and infiltrating changes like edema. Preliminary results on five cases presenting tumor types with very different characteristics demonstrate the potential of the new technique for clinical routine use for planning and monitoring in neurosurgery, radiation oncology, and radiology.**

## I. Introduction

Segmentation of medical images, as opposed to natural scenes, has the significant advantage that structural and intensity characteristics are well known up to a natural biological variability or the presence of pathology. Most common is pixel- or voxel-based statistical classification using multiparameter images [1], [2]. These methods rely on the properties of single voxels and do not consider global shape and boundary information. Applied to brain tumor segmentation, classification approaches have met with only limited success [3], [4] due to overlapping intensity distributions of healthy tissue, tumor, and surrounding edema. Often, lesions or tumors were considered as outliers of a mixture Gaussian model for the global intensity distribution, [5], [6], [7], assuming that lesion voxels are distinctly different from normal tissue characteristics.

Warfield et al. [8], [9] combined elastic atlas registration with statistical classification. Elastic registration of a brain atlas helped to mask the brain from surrounding structures. A further step uses "distance from brain boundary" as an additional feature to improve separation of clusters in multi-dimensional feature space. Initialization of probability density functions still requires a supervised selection of training regions. The core idea, namely to augment statistical classification with spatial information to account for the overlap of distributions in intensity feature space, is part of the new method presented in this paper.

Leemput et al. [10], [11] developed fully automatic segmentation of MR head images by statistical classification using an atlas prior both for initialization of probability density functions and also for geometric constraints, solved as an expectation maximization (EM) algorithm. The method has been shown to be very robust and highly reproducible for normal brain images, but fails in the presence of large pathology. A most recent extension detects brain lesions as outliers [12] and was successfully applied for detection of multiple sclerosis lesions. Brain tumors, however, can't be simply modelled as intensity outliers due to overlapping intensities with normal tissue and/or significant size.

We propose a fully automatic method for segmenting MR images presenting tumor and edema, both mass-effect and infiltrating structures. This method builds on the previously published work done by [10], [11]. Additionally, tumor and edema classes are added to the segmentation. The spatial atlas that is used as a prior in the classification is modified to include prior probabilities for tumor and edema. As with the work done by other groups, we focus on a subset of tumors to make the problem tractable. Our method provides a full classification of brain tissue into white matter, grey matter, cerebrospinal fluid (csf), tumor, and edema. Because the method is fully automatic, it is fully reproducible.

## II. Expectation Maximization segmentation

An algorithm for fully automatic segmentation of normal brain tissue using an Expectation Maximization (EM) algorithm has been previously developed by [10], [11]. This algorithm estimates both the probability distributions of the tissue classes (gray matter, white matter, and csf), and the intensity inhomogeneity or bias field.

Each tissue class is modelled by a normal distribution. The bias field, which is known to be multiplicative, is made to be additive by computing the logarithmic transformation on the intensities. The bias is modelled by a polynomial $\sum_k C_k \phi_k(x)$. The probability that a voxel with value

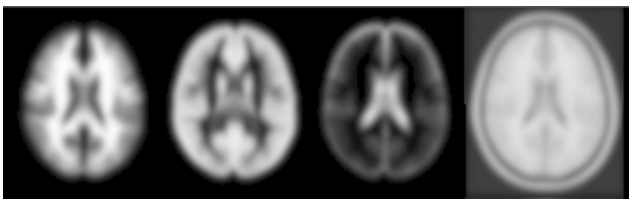

Fig. 1. SPM atlas providing spatial probabilities. From left to right: white matter, gray matter, csf, template T1 image for registration.

$y_i$ belongs to class $j$ is then

$$p(y_i|\Gamma_i = j, \theta_j, C) = G_{\sigma_j}(y_i - \mu_i - \sum_k C_k \phi_k(x_i)), \quad (1)$$

where $\Gamma_i$ is the tissue class of the voxel at position $i$, $\theta_j = \mu_j, \sigma_j$ is the distribution parameters for class $j$, and $C = C_k$ is the bias field parameters.

The Expectation Maximization segmentation (EMS) algorithm interleaves probability distribution estimation for each tissue class, classification, and bias field correction using the classic EM approach. The probability distributions are initialized using the digital brain atlas. The algorithm then iteratively

1. classifies the MR data using the current probability distribution and bias field estimates,
2. updates the bias field estimate using the classification,
3. re-estimates the probability distributions from the bias corrected data

until the probability distributions converge. The equation for the classification step is

$$p(\Gamma_i = j|y_i, \theta) = \frac{p(y_i|\Gamma_i = j, \theta_j)p(\Gamma_i = j)}{\sum_k p(y_i|\Gamma_i = k, \theta_k)p(\Gamma_i = k)} \quad (2)$$

The expressions for the parameters $\mu_j$ and $\sigma_j$ are

$$\mu_j = \frac{\sum_i p(\Gamma_i = j|y_i, \theta, C)(y_i - \sum_k C_k \phi_k(x_i))}{\sum_i p(\Gamma_i = j|y_i, \theta, C)} \quad (3)$$

and

$$\sigma_j^2 = \frac{\sum_i p(\Gamma_i = j|y_i, \theta, C)(y_i - \mu_j - \sum_k C_k \phi_k(x_i))^2}{\sum_i p(\Gamma_i = j|y_i, \theta, C)} \quad (4)$$

The bias field estimation uses the intermediate classification and Gaussian distribution estimates. A prediction of the signal without bias is constructed from the current classification and distribution estimates, and subtracted from the original signal. A weight is assigned each voxel in the residue image inversely proportional to a weighted variance. The bias field is then estimated as a weighted least-squares fit from the residue image.

The EMS algorithm uses a spatial atlas from the Statistical Parametric Mapping (SPM) package for initialization and classification. The SPM atlas contains spatial probability information for brain tissues. It was created by averaging hand segmentations of normal patients that had been registered by an affine transformation (Fig. 1).

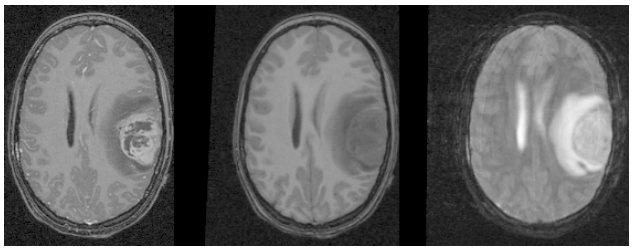

Fig. 2. Registered dataset showing a malignant glioma. From left to right: T1 post-contrast, T1 pre-contrast, T2. The tumor (mostly) enhances with contrast agent in the post-contrast image. Also note the edema surrounding the tumor.

This spatial atlas is used to initialize the distribution estimates before the first EM iteration. The atlas is registered to the patient data, with an affine transformation, providing spatial prior probabilities for the tissue classes. The distribution estimates are then calculated based on the atlas probabilities. This allows the algorithm to be fully automatic.

The atlas is also used as the prior probability $p(\Gamma_i = j)$ during the classification step (Equation 2). For normal brains, this makes the algorithm more robust to noise and intensity inhomogeneity.

## III. Tumor characteristics

It is important to understand the characteristics of tumors before attempting to develop an algorithm for tumor segmentation from MR images. Some of the general characteristics of brain tumors are that they

- vary greatly in size and position,
- vary greatly in the way they show up in MRI,
- may have overlapping intensities with normal tissue,
- may be space occupying (new tissue that moves normal structure) or infiltrating (changing properties of existing tissue),
- may enhance fully, partially, or not at all, with contrast agent,
- may be accompanied by surrounding edema.

When a dataset contains a tumor (see Fig. 2), several problems are immediately apparent with the EMS algorithm described in section II.

First, the atlas used does not contain a spatial prior for tumor tissue. The atlas is a normal brain atlas, and cannot be used directly in the presence of pathology. When the atlas is used as a spatial prior for tissue classification, all brain tissue must be classified as either white matter, gray matter, or csf. The results of using the normal brain atlas on the dataset in Fig. 2 is shown in Fig. 3. The tumor tissue is classified as one of the available tissue types, mostly csf in this case.

Second, tumors are often accompanied by edema, which is a swelling of normal tissue surrounding the tumor, and which changes the tissue properties in that area. The amount and regional extent of edema that accompanies a tumor is variable. Edema or infiltrating phenomena in general are also not explained by the SPM atlas.

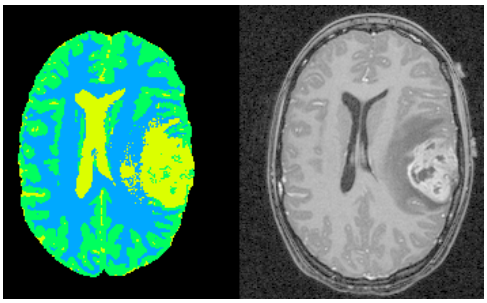

Fig. 3. Segmented dataset using normal brain atlas, with T1 post-contrast image for reference. Blue = white matter, green = grey matter, yellow = csf.

## IV. Assumptions used for EMS extension

As one would expect, making certain assumptions and using prior information can help greatly in the problem of segmenting brain tumors. We make some important simplifying assumptions for our segmentation framework.

**Tumor characteristics:** We assume that tumors are ring-enhancing or fully enhancing with contrast agent. The major tumor classes that fall in this category, and hence are the tumor types that we have focused on, are meningiomas and malignant gliomas. The basic characteristics of *meningiomas* are a) smooth boundaries b) normally space occupying and c) smoothly and fully enhancing with contrast agent. The basic characteristics of *malignant gliomas* are a) ragged boundaries, b) initially only in white matter, possibly later spreading outside white matter, c) margins enhance with contrast agent, inside doesn't, d) accompanied by edema, and e) infiltrating at first, possibly becoming space occupying when larger.

**MR sequences:** We assume that all datasets analyzed include a T1 pre-contrast image, a T1 post-contrast image (both with $1x1x1.5mm^3$ voxel dimensions), and a T2 image ($1x1x3mm^3$ voxel dimensions) (Fig. 2). This inter-slice spacing is the standard protocol at the hospitals where our datasets were acquired. All of our data are acquired on Siemens 1.5T and Siemens 3T MRI scanners.

## V. Extension of the EMS algorithm

**Tumor class:** In addition to the three tissue classes assumed in the EMS segmentation (white matter, grey matter, csf), we add a new class for tumor tissue. Whereas the (spatial) prior probabilities for the normal tissue classes are defined by the atlas, the spatial tumor prior, $p(\Gamma_i = j)$, is calculated from the T1 pre- and post-contrast difference image. The histogram of the difference image shows a peak around 0, corresponding to noise and subtle misregistration, and some positive response corresponding to gadolinium enhancement. We calculate a mixture model fit of two continuous distributions (Gaussian and Gamma functions) to fit the difference image histogram. The posterior probability of the gadolinium enhancement distribution is then used to map the difference image to a prior probability image for tumor. We also maintain a low base probability (0.05) for the tumor class across the whole brain region

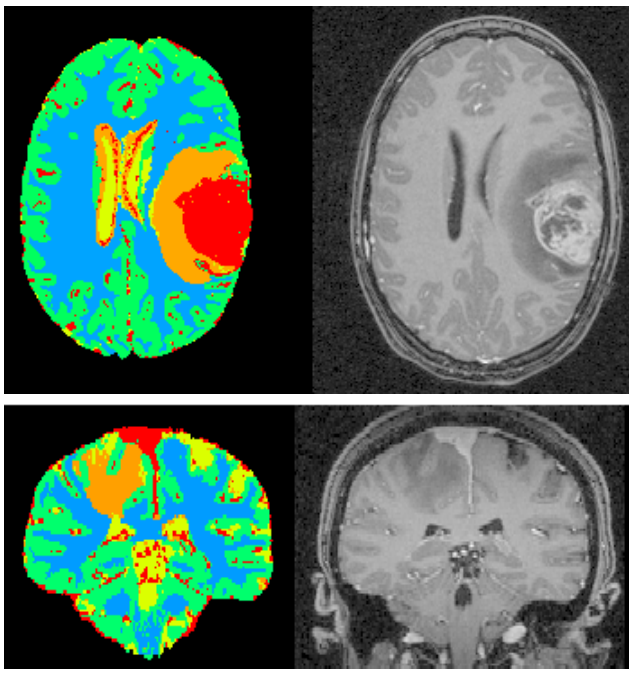

Fig. 4. Two segmented datasets containing malignant glioma (top) and meningioma (bottom), with T1 post-contrast images for reference. Blue = white matter, green = grey matter, yellow = csf, orange = edema, red = tumor.

to account for tumor tissue that does not enhance with contrast.

The normal tissue priors are scaled appropriately to allow for this new tumor prior, so that the probabilities still sum to 1. This forces tissue that enhances with gadolinium to be included in the tumor class, and prevents enhancing tissue from cluttering the normal tissue classes.

The gadolinium enhanced T1 image is not used as a channel for classification but only provides a spatial prior through the difference image. Thus, it controls the initialization of the multivariate probability density function for tumor. This strategy is reasonable because the gadolinium enhanced channel does not provide any extra information except what the difference image provides.

**Edema class:** We also add a separate class for edema. We have found that edema, when present, is most evident in white matter. We create an edema class prior that is a fraction of the white matter prior probability. The other priors are scaled to allow for the edema prior, just as for the tumor prior. During initialization, we calculate the estimate for edema using the modified atlas prior, just as for the other classes, but then we modify the mean value for edema to be between white matter and csf, which is how edema appears in T1 and T2 weighted images (see Fig. 2).

## VI. Results

We have applied our tumor segmentation framework to five different datasets, including a wide range of tumor types and sizes. All datasets were registered to the SPM atlas using mutual information registration as described by [13]. Fig. 4 shows results for two datasets.

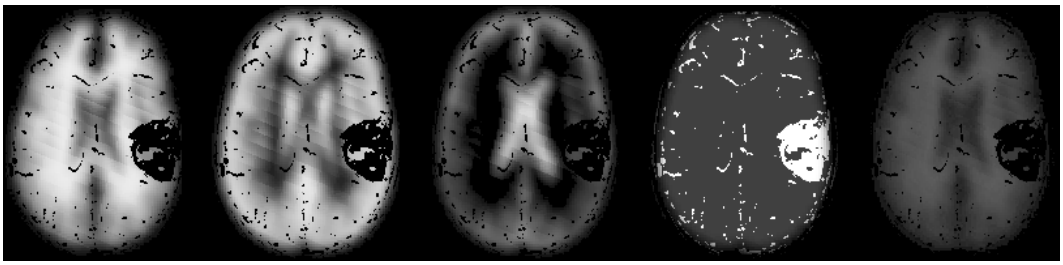

Fig. 5. Spatial prior for the dataset in Fig. 2, created from the SPM atlas and the T1 pre- and post-gad difference image. From left to right: white matter, grey matter, csf, tumor, edema.

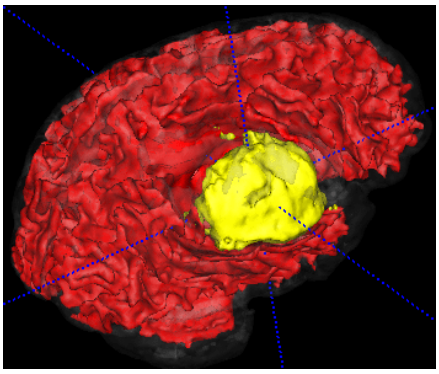

Fig. 6. Three-dimensional rendering of segmented tumor (yellow), white matter tissue (red) and surrounding cortical gray matter (light gray).

Fig. 5 shows the resulting atlas used for classification of the dataset in Fig. 2 with the additional tumor and edema channels.

## VII. Conclusions

We have developed a model-based segmentation method for segmenting head MR image datasets with tumors and infiltrating edema. This is achieved by extending the spatial prior of a statistical normal human brain atlas with individual information derived from the patient's dataset. Thus, we combine the statistical geometric prior with image-specific information for both geometry of newly appearing objects, and probability density functions for healthy tissue and pathology. Applications to five tumor patients with variable tumor appearance demonstrated that the procedure can handle large variation of tumor size, interior texture, and locality. The method provides a good quality of healthy tissue structures and of the pathology, a requirement for surgical planning or even image-guided surgery (see Figs. 4 and 6). Thus, it goes beyond previous work that focuses on tumor segmentation only.

Currently, we are testing the validity of the segmentation system in a validation study that compares resulting tumor structures with repeated manual experts' segmentations, both within and between multiple experts.

In our future work, we will study the issue of deformation of normal anatomy in the presence of space-occupying tumors. Within the range of tumors studied so far, the soft boundaries of the statistical atlas (see Fig. 1) could handle spatial deformation. However, we will develop a scheme for high dimensional warping of multichannel probability data to get a better match between atlas and deformed patient images.

### A. Acknowledgments

This work was supported by NIH-NCI R01CA67812.

## References

[1] M. Just and M. Thelen, "Tissue characterization with t1, t2, and proton density values: Results in 160 patients with brain tumors," *Radiology*, , no. 169, pp. 779–785, 1988.

[2] G. Gerig, J. Martin, R. Kikinis, O. Kubler, M. Shenton, and F.A. Jolesz, "Automating segmentation of dual-echo MR head data," in *Lect Notes Comp Sci*, 1991, vol. 511, pp. 175–185.

[3] R.P. Velthuizen, L.P. Clarke, S. Phuphianich, L.O. Hall, A.M. Bensaid, J.A. Arrington, H.M. Greenberg, and M.L. Siblinger, "Unsupervised measurement of brain tumor volume on mr images," *JMRI*, , no. 5, pp. 594–605, 1995.

[4] S. Vinitski, C. Gonzales, F. Mohamed, T. Iwanaga, R.L. Knobler, K. Khalili, and J. Mack, "Improved intracranial lesion characterization by tissue segmentation based on a 3d feature map," *Mag Re Med*, , no. 37, pp. 457–469, 1997.

[5] M. Kamber, R. Shingal, D.L. Collins, D.S. Francis, and A.C. Evans, "Model-based, 3-D segmentation of multiple sclerosis lesions in magnetic resonance brain images," *IEEE-TMI*, , no. 14, pp. 442–453, 1995.

[6] A. Zijdenbos, A. Evans, F. Riahi, J. Sled, H.C. Chui, and V. Kollokian, "Automatic quantification of multiple sclerosis lesion volume using stereotaxic space," *VBC*, pp. 439–448, 1996.

[7] A. Zijdenbos, R. Forghani, and A. Evans, "Automatic quantification of ms lesions in 3d mri brain data sets: Validation of insect," in *Lect Notes Comp Sci*, 1998, vol. 1496, pp. 439–448.

[8] S. Warfield, J. Dengler, J. Zaers, C.R.G. Guttman, W.M. Wells, G.J. Ettinger, J. Hiller, and R. Kikinis, "Automatic identification of gray matter structures from mri to improve the segmentation of white matter lesions," *MICCAI*, vol. 1, no. 6, pp. 326–338, 1996.

[9] S. Warfield, M. Kaus, F.A. Jolesz, and R. Kikinis, "Adaptive template moderated spatially varying statistical classification," in *MICCAI*, William M. Wells, Alan Colchester, and Scott Delp, Eds. Oct 1998, vol. 1496 of *Lecture Notes in Computer Science*, pp. 431–438, Springer.

[10] K. Van Leemput, F. Maes, D. Vandermeulen, and P. Suetens, "Automated model-based tissue classification of MR images of the brain," *IEEE TMI*, vol. 18, pp. 897–908, October 1999.

[11] K. Van Leemput, F. Maes, D. Vandermeulen, and P. Suetens, "Automated model-based bias field correction of MR images of the brain," *IEEE TMI*, vol. 18, pp. 885–896, October 1999.

[12] K. Van Leemput, F. Maes, D. Vandermeulen, A. Colchester, and P. Suetens, "Automated segmentation of multiple sclerosis lesions by model outlier detection," *IEEE TMI*, vol. 20, pp. 677–688, August 2001.

[13] F. Maes, A. Collignon, D. Vandermeulen, G. Marchal, and P. Seutens, "Multi-modality image registration by maximization of mutual information," *IEEE-TMI*, , no. 16, pp. 187–198, 1997.